A novel method for 3D face symmetry reference plane based on Weighted Procrustes Analysis algorithm

Zhu Yujia
Peking University School of Stomatology https://orcid.org/0000-0001-9234-5783
Shengwen Zheng
Beijing University of Posts and Telecommunications
Guosheng Yang
Beijing University of Posts and Telecommunications
Xiangling Fu
Peking University of Posts and Telecommunications
Yijiao Zhao (kqcadcs@bjmu.edu.cn)
Yong Wang
Peking University School of Stomatology

Research article

Keywords: Symmetry Reference Plane, Procrustes Analysis, three-dimensional facial data, mandibular deviation, anatomic landmarks

Posted Date: June 15th, 2020

DOI: https://doi.org/10.21203/rs.3.rs-31980/v1

Version of Record: A version of this preprint was published on November 11th, 2020. See the published version at https://doi.org/10.1186/s12903-020-01311-3.

Abstract

Background

We aimed to establish a novel method based on Weighted Procrustes Analysis (WPA) algorithm that assigns weight to facial anatomical landmarks to automatically construct a three-dimensional facial Symmetry Reference Plane (SRP) for mandibular deviation patients.

Methods

Three-dimensional facial SRPs were extracted independently from 15 mandibular deviation patients, using both our WPA algorithm and the standard PA algorithm. A reference plane defined from professional experience served as the ground truth. To test whether the WPA SRP or the PA SRP was closer to the ground truth, we measured the position error of mirrored landmarks, the facial asymmetry index (FAI) error, and the angle error for the global face and for each facial third partitions.

Results

The average angle error between the WPA SRP and the ground truth was 1.66 ± 0.81°, which was smaller than that between the PA SRP and the ground truth. The position error of mirrored landmarks constructed using the WPA algorithm in the global face (3.64 ± 1.53 mm) and each facial partition was lower than the error of those constructed using the PA algorithm. The average FAI error of the WPA SRP was − 7.77 ± 17.02 mm, which was smaller than that of the PA SRP.

Conclusions

This novel automatic algorithm based on weighted anatomic landmarks provided a more adaptable SRP than the standard PA algorithm when applied to severe mandibular deviation patients and better simulated the diagnosis strategy of clinical experts.

1. Background

Facial asymmetry is characterised by multiple features and forms, of which mandibular deviation is one of the more common manifestations, accounting for 70%–80% of all facial asymmetry cases[1–3]. The restoration of symmetrical, coordinated, and aesthetic facial shapes is a central goal of oral and maxillofacial surgery, orthodontics and prosthodontics[4–6]. With the widespread application of three-dimensional digital technology, the extraction of the symmetry reference plane (SRP) is the primary step in the symmetry analysis of three-dimensional facial data[7]. The accuracy of the SRP directly affects the symmetry index and is critical both for developing a clinical treatment plan and evaluating treatment effects.

The traditional methods for extracting an SRP are often based on medical and bilateral anatomical landmarks measured either on a digital three-dimensional facial model or with the head in a natural position[8–12]. These methods are widely used, but landmarks are defined differently by different scholars, which makes it difficult to establish common methods suitable for addressing different types of facial asymmetry[13, 14]. In recent years, a method of extracting the SRP based on superimposed three-dimensional original and mirror facial data (referred to as the original-mirror alignment method) has received increased attention.

The original-mirror alignment method involves superimposing the three-dimensional geometric shape of the facial model (the original model) onto its mirror model[15]. The SRP of the original model is determined by analysing the symmetry planes of the superimposed model, which is geometrically symmetrical. The core step of this method is the three-dimensional superimposition, which mainly involves the iterative closest point (ICP) and Procrustes Analysis (PA) algorithms[16, 17]. The ICP algorithm seeks the optimal superimposed position of the three-dimensional original and mirror models composed of tens of thousands of point clouds determined by an iterative solution[18]. Based on the one-to-one relationship between the original and mirror landmarks (usually anatomical landmarks), the PA algorithm obtains the superimposed position with the minimum average distance between the two sets of landmarks through a matrix operation to obtain the optimal superimposed position of the original and mirror models[19]. The significant difference between the PA and ICP algorithms is that SRP extraction using the PA algorithm relies more on anatomical facial landmarks. Furthermore, the PA algorithm is more aligned with stomatological clinical diagnosis and treatment and has thus received widespread attention in recent years.

In 2015, Xiong et al. reported an application of the PA algorithm that extracts the facial SRP using 21 important anatomical landmarks[20]. While this algorithm is suitable for normal facial data, it is not ideal for facial asymmetry data (particularly data from patients with complex facial deformities) because the algorithm lacks a mechanism for assigning weights to individualised facial features (different degrees of asymmetry), and there is still a discrepancy between the algorithm results and the logical basis of oral clinical diagnosis[21].

Based on standard PA algorithm research, this study aims to establish a Weighted Procrustes Analysis (WPA) algorithm for extracting a three-dimensional facial SRP that can automatically recognise the weight assignment of facial landmarks. Our study analysed and evaluated the WPA algorithm suitability for commonly seen clinical cases of mandibular deviation.

2. Methods

2.1 Subjects

Fifteen patients from the Department of Oral and Maxillofacial Surgery, Orthodontics and Prosthodontics at the Peking University School and Hospital of Stomatology were recruited for this study. The inclusion

criteria were as follows: an apparent facial asymmetry with a mandibular deviation of at least 3 mm from the facial midline, which is perpendicular to the interpupillary line at the soft tissue nasion when the patient is seated with a natural head position. The exclusion criteria were a history of previous craniofacial trauma, orthognathic surgery, orthodontic treatment or congenital anomalies. This research was approved by the bioethics committee of the Peking University School and Hospital of Stomatology (PKUSSIRB-20163113) and was carried out in accordance with approved guidelines and regulations for research involving human subjects. All participants were fully informed of the experimental purpose and procedure and signed an informed consent document before the experiments commenced.

2.2 Experimental equipment and software

A Face Scan 3D sensor system (3D-Shape Corp, Germany, Erlangen) was used to collect three-dimensional facial data from each patient. We obtained the facial data in only 0.2–0.8 s with high accuracy in the z-direction (0.1 mm). The scanning range was 270°–320°, the imaging principle was raster scanning using 5 million CCD (charge-coupled device) pixels, and the approximate number of large points was 10 000.

For data processing, we used the reverse engineering software Geomagic Studio 2013 (3D System, USA, Morrisville), which is used to process three-dimensional facial data and conduct SRP extraction. The WPA algorithm developed in this study was based on the Python programming language, which optimises the objective function of the PA algorithm by assigning weights. The formula for the weight factor Wi is shown in formula □, and the WPA objective function F' is shown in formula □.

$$w_i = \frac{1}{\|LMK\_Org - LMK\_Mir\|_2} \quad ①$$

$$F' = \min_{Q} \sum_{i=1}^{p} \mathrm{w_i} \|\mathrm{LMK\_Orgi} - \mathrm{QLMK\_Miri}\|_2 \quad ②$$

Where Wi (i = 1,2, ..., 32) is the weight factor for each facial landmark (assigned according to the degree of asymmetry of the landmarks), LMK_Org is the original model landmark set, LMK_Mir is the mirror model landmark set, LMK_Orgi and LMK_Miri (i = 1,2, ..., n) are the corresponding landmarks in the original and mirror landmark set, respectively, Q is the spatial change matrix, and p is the number of landmarks.

2.3 Data capturing and processing

When acquiring the three-dimensional facial data, we calibrated the equipment before use to ensure accurate image acquisition. The patient was guided by the clinician to a natural head position at distance of 135 cm from the scanner and a sitting position with both eyes looking forward, keeping the Frankfort horizontal (FH) plane parallel to the floor. Data was obtained when the facial expression was naturally relaxed. The criteria that were implemented for the face scan data were an effective display of facial contours, a high-resolution image, no obvious movement, and a closed mouth.

Geomagic Studio 2013 was used to process the image, which included removing extra data, smoothing the shells, and filling small holes. The original three-dimensional facial model was adjusted to the natural head position so that the FH plane of the natural head position coincided with the XZ plane of the global coordinate system and the sagittal plane coincided with the YZ plane of the global coordinate system. Three experienced clinical senior professors completed the extraction of anatomical landmarks from each original facial model (Model_Org). Thirty-two anatomical landmarks were selected from the overall region, including the glabella, nasion, pogonion, and alare et al.. An example of a selected landmark is depicted in Fig. 1. Each researcher performed the extraction three times and calculated the mean coordinate value of the original landmark (LMK_Org). Next, the centre of gravity of the original model was moved to the origin of the global coordinate system, and the data was saved in a .OBJ file.

2.4 Abstracting the SRP

2.4.1 Initial alignment of the original and mirror model

For each of the 15 case models in this study, the original model (Model_Org) was initially superimposed onto its YZ-plane mirror model, in order to obtain an ideal weight distribution of the 32 PA landmarks. Geomagic Studio 2013 software was used for the Global ICP registration function. During the process, the original model was fixed, and the mirror model was floated. The mirror model (Model_Mir) was obtained after superimposition, and the corresponding initial mirror landmarks were then established (LMK_Mir).

2.4.2 Control group: abstracting the SRP with the PA algorithm

The three-dimensional coordinates of all landmarks in the original and mirror images (LMK_Org and LMK_Mir; 32 pairs of landmarks in total) were derived and entered into the PA algorithm program, which was based on the Python language, without weight differences. The transformation matrix of the mirror model was then calculated and loaded onto Model_Mir using Geomagic Studio 2013. Finally, the SRP of the facial data for each of the 15 patients was constructed by taking the union of the original and mirror models (Model Uni_PA) and defined as ‘SRP_PA’.

2.4.3 Test group: abstracting the SRP with the WPA algorithm

Similarly, the three-dimensional coordinates of all landmarks in the original and mirror images (LMK_Org and LMK_Mir; 32 pairs of landmarks in total) were derived and entered into the WPA algorithm program, which was based on the Python language. The weight factor for each landmark was calculated automatically according to the distance of paired landmarks. For example, a landmark pair with good symmetry would be relatively close together after initial registration and would thus be given more weight. Conversely, a landmark pair with poor symmetry would be relatively far apart and would thus be given less weight.

The weighted landmarks of LMK_Org and LMK_Mir were superimposed three-dimensionally based on the least-weighted squares, so that optimal superimposition was obtained for the 32 pairs of landmarks and the WPA transformation matrix of the mirror model (Model_Mir) was derived. The transformation matrix was loaded onto Model_Mir using Geomagic Studio 2013. Finally, the SRP of the facial data for each of the 15 patients was constructed by taking the union of the original and mirror models (Model Uni_WPA) and defined as 'SRP_WPA'.

2.4.4 Professional group: abstracting the ground truth

Studies have shown that the alignment of the original and mirror models for SRP abstraction based on areas defined by experts to have good symmetry exhibits sufficient adaptability for facial asymmetry cases, but the reliance on expert definitions has led to a reduced degree of algorithm automation. The SRP of an algorithm based on professional expertise and empirical data was regarded as the ground truth in this study. Regions with good facial symmetry from the original and mirror models (Model_Org and Model_Mir) were manually selected by senior doctors using Geomagic Studio software, and regional registration was carried out with the two models (Model_Org fixed and Model_Mir floated). Finally, the SRP of the facial data for each of the 15 patients was constructed by taking the union of the original and mirror models (Model Uni_Pro). These SRPs were defined as the ground truth ('SRP_Pro').

The SRPs constructed using the WPA, PA, and professional algorithms are shown in Fig. 2.

2.5 SRP measurement evaluation

2.5.1 Angle error of planes

For each of the 15 three-dimensional mandibular deviation models, the angles between SRP_PA and SRP_Pro and between SRP_WPA and SRP_Pro were calculated and recorded as Err_Ang_PA and Err_Ang_WPA, respectively. The average and standard deviation of the angle error for each sample were also calculated.

2.5.2 Position error of the mirrored landmarks

The position error of the mirrored landmarks was defined as a new quantitative index to evaluate the SRP, which may further validate the result of the weighted landmarks. The position error indicator was designed to obtain the weight distribution of the WPA algorithm landmarks and professional landmarks (implied empirical information) by calculating the distance between corresponding landmarks in the WPA and professional algorithms. If the two weights are consistent, then the mirror landmark overlap is suitable, and the position error is small. Conversely, if the weights are inconsistent, then the position error is large. The mean value of the position error reflects the consistency between the SRPs of the WPA and professional algorithms in accounting for the weight distribution of the global facial landmarks.

The mirror landmarks of each model (LMK_Mir_PA and LMK_Mir_WPA) were obtained from the mirror and original models using the SRP_PA and SRP_WPA, and the mirror landmarks of the professional group

(LMK_Mir_Pro) were similarly obtained. The global position error was defined as the average distance of the 32 pairs of landmarks in LMK_Mir_PA and LMK_Mir_Pro and in LMK_Mir_WPA and LMK_Mir_Pro. In this process, the original model was fixed in the control group, test group, and professional group. The closer each mirror landmark constructed by the SRPs of the test and control groups was to the same landmark in the professional group (the smaller the position error), the closer we considered the SRP to be to the professional plane. The global position error was calculated based on 32 paired landmarks (Err_LMK_WPA and Err_LMK_PA) (Fig. 3).

The Severt study showed that the frequency of asymmetry is 5% in the upper facial region, 36% in the middle, and 74% in the lower[22]. For mandibular deviation patients, the degree of asymmetry of landmarks in the lower part of the face is significantly higher than those in the middle and upper parts. Therefore, the weight distribution of features in different regions should be different and cannot be analysed with the global position error. Thus, we also evaluated the regional position error of the three facial partitions. The regional position error was calculated for landmarks in each facial third partitions: 4 landmarks in the upper third, 17 in the middle third, and 11 in the lower third, named Err_LMK_WPA_Up and Err_LMK _PA_Up, Err_LMK_WPA_Mid and Err_LMK _PA_Mid, and Err_LMK_WPA_Low and Err_LMK _PA_Low, respectively. The average and standard deviation of the global and regional position error were calculated for each of the 15 samples.

2.5.3 FAI error

The FAI error was calculated based on the SRP constructed for the test and control groups of the 15 facial datas and defined as the sum of the distance from the medical landmark to the SRP and the difference between bilateral landmarks and the SRP. The FAI_PA, FAI_WPA, and FAI_Pro were obtained according to formula ③. Err_FAI_WPA and Err_FAI_PA were defined as the difference between the FAI values of the WPA and professional algorithm and the difference between the FAI values of the PA and professional algorithm, respectively. The average value and standard deviation of the FAI error of each of the 15 samples were calculated.

$$FAI = \sum_{i=1}^{10} Md_i + \sum_{i=1}^{11} |Rd_i - Ld_i| \qquad ③$$

Md_i represents the distance from the medical landmark to the SRP. Rd_i and Ld_i represent the differences between the right landmark and the SRP and that between the left landmark and the SRP, respectively.

2.6 Statistical analysis

Statistical analysis was performed with SPSS software (Version 21, SPSS Inc., Chicago, IL, USA). A K-S normality test was conducted for the angle error (of two groups), the global position error (of two groups), the regional position error (of six groups), and the FAI error (of two groups) to examine the distribution of the data (there were 15 calculated values for each group).

The workflow of experimental procedures and evaluation methods is shown in Fig. 4. We performed a paired *t*-test analysis of the position error of both the WPA and PA algorithm groups of 15 patients to evaluate the overlapping difference of the WPA and PA algorithms in terms of global and regional landmarks. The statistical significance was set at $P < 0.05$.

A one-way ANOVA analysis was performed of regional landmarks of position error to examine whether differences in the position error of different facial partitions were statistically significant. A homogeneity-of-variance test was also performed. Tukey's honesty significance test was used to perform multiple comparisons. The statistical significance was set at $P < 0.05$. A paired *t*-test analysis was also conducted to compare the angle error and FAI error.

3. Results

3.1 Analysis of angle error

The K-S normality test for angle error (of two groups of 15 values each) revealed that both groups conformed to the normal distribution. Data analysis yielded no statistically significant differences ($P > 0.05$) between the PA and WPA algorithm groups. Measurement analysis showed that the mean and standard deviation of the angle error in the PA and WPA groups were 2.16 ± 1.08° and 1.66 ± 0.81°, respectively. Since the mean and standard deviation of the angle error of the WPA algorithm group were smaller, this indicates that the SRP constructed using the WPA algorithm for the 15 data points was closer to the ground truth plane.

3.2 Analysis of position error

Table 1 reports the measurement values for the position error between the test and control groups for global landmarks (two groups of 15 values each) and regional landmarks (six groups of 15 values each). The K-S normality test for position error revealed that all groups conformed to the normal distribution. There were significant differences in the position errors among the groups ($P < 0.05$).

Tukey's honesty significance test revealed statistically significant differences ($P < 0.05$) between the lower and upper facial partitions in the WPA group, between the lower and upper partitions in the PA group, and between the lower and middle partitions in the PA group. Related sample data distribution and statistical analysis results are shown in Fig. 4.

The measurement results of the position error are shown in Table 1.The mean and standard deviation of the global position error of the WPA and PA groups were 3.64 ± 1.53 mm and 4.54 ± 1.92 mm, respectively; the mean and standard deviation of the position error of the WPA algorithm group were smaller than those of PA group. Among the six groups of regional facial data, the position errors of the upper, middle, and lower partitions in the WPA group were 2.38 ± 1.15 mm, 3.27 mm ± 1.29 mm, and 4.63 ± 2.28 mm, respectively; the position error was lowest in the upper partition. The difference between the lower partition error and the global mean position error was 0.99 mm.

In the PA group, the position errors of the upper, middle, and lower partitions were 3.67 ± 1.84 mm, 3.77 ± 1.51 mm, and 6.35 ± 3.23 mm; the position error was highest in the lower partition. The difference between the lower partition error and the global mean position error was 1.81 mm. These results showed that the global error and regional error of the WPA group were smaller than those of the PA group and that the lower partitions weighted overlap result of the WPA group was closer than that of the PA group to the weighted overlap result of the professional group, showing a significant improvement in the WPA group compared with the PA group.

3.3 Analysis of FAI error

The K-S normality test for FAI error (in two groups of 15 values each) revealed that both groups conformed to the normal distribution. Data analysis yielded no statistically significant differences ($P > 0.05$) between the PA and WPA groups. There were no significant differences between the FAI errors of the two groups ($P > 0.05$). Measurement analysis showed that the average FAI errors calculated with the WPA and PA algorithms were 13.65 ± 12.45 mm and 15.77 ± 14.32 mm, respectively. The result of the WPA-calculated SRP was closer than the PA-calculated SRP to the SRP of the ground truth plane.

4. Discussion

4.1 The WPA SRP was more closely aligned than the standard PA SRP with the ground truth plane

The weighted algorithm is an important innovation of this study, the degree of symmetry of the landmarks could be evaluated quantitatively and used as landmark weight factors to construct an SRP. Our WPA algorithm, is designed to assign a small weight for landmarks with poor symmetry after the initial global ICP superimposition of the original and mirror models and a large weight for landmarks with good symmetry. The weight calculation method is based on the reciprocal of the distance between the paired landmarks, which reflects the inverse relationship between the distance and the corresponding assigned weight. Based on superimposition using least-weighted squares, all original and mirror PA landmarks were assigned different weights, the solution to the PA landmark set system (the WPA objective function) was minimised. As a result, the optimal overlap result of the original and mirror landmarks was achieved.

The results indicated that the average angle error of WPA group for the 15 patients with mandibular deviation was less than 2°, and although there was no statistically significant result when compared with the average angle error of the standard unweighted PA algorithm (of which the error was greater than 2°), the result of the WPA SRP was closer to the ground truth (Fig. 2), and the angle error displayed a downward trend.

Jia Wu et al. showed that the angle difference between the two planes is easily perceived when it is more than 6°[23]. The angle error between the WPA SRP and the professional plane was less than 2°, which indicates that the accuracy of the WPA SRP was almost equal to that of the professional plane and therefore had better clinical suitability than the PA SRP. Furthermore, the stability level of the WPA

algorithm, with a standard deviation of 0.81°, was significantly higher than that of the PA algorithm, which had a standard deviation of 1.08°.

Additionally, the FAI value calculated for the WPA algorithm was closer to the professional result than was the FAI value calculated for the PA algorithm. Furthermore, the WPA FAI for patients with mandibular deviation was also closer to the ground truth plane than was the PA FAI. These results confirmed that the WPA algorithm performed better than the PA algorithm in constructing facial SRPs for facial asymmetry (mandibular deviation).

4.2 A new SRP evaluation indicator: the position error of mirror landmarks

In previous studies of SRPs of the face and skull, SRP evaluation indicators have mainly included the angle error and FAI error[24, 25]. These two indicators can assess the global proximity of the SRP, but neither can quantitatively analyse facial landmark asymmetry. In this study, we proposed to use the position error indicator as a novel SRP evaluation tool.

The mirror landmarks differed between the test and professional SRPs for mirroring the original facial model, while the original model was the same between the test and professional groups. The results in Table 1 indicate that the mean values of the global position errors of the WPA and PA algorithms were 3.64 mm and 4.54 mm, respectively, and that the difference between the two was statistically significant. This indicates that the global overlapping degree of the WPA algorithm mirrored features and professional mirrored features was more accuracy than that of the PA algorithm. The weight distribution of the WPA algorithm was also significantly more accurate than that of the PA algorithm; the weight factor of the WPA algorithm had a significant effect.

The mean value of the regional position error for the upper, middle, and lower partitions also reflected the degree of consistency between the weight distribution of the WPA SRP and the professional SRP for each facial partition. The mean position error of the WPA algorithm was smaller than that of the PA algorithm for all three facial partitions. This difference was statistically significant, indicating that the WPA algorithm for each facial partition was close to the professional algorithm.

Additionally, the position error of the WPA algorithm for the upper and lower parts of the face was considerably smaller than that of the PA algorithm, while that for the middle part of the face was close to that of the PA algorithm. This occurred because the WPA algorithm allocated a lower weight for lower facial landmarks to reduce their influence on the global overlapping degree, while the upper landmarks were assigned higher weights to increase the overlapping degree, thus accounting for professional experience in the weight distribution of the landmarks. Compared with the PA algorithm without weight distribution, the position error of the WPA in each region was optimised, and an ideal SRP construction result was obtained.

4.3 Limitations and further research to improve the three-dimensional facial SRP

Previous research on the original-mirror alignment method is mainly divided with regard to the use of the ICP and PA algorithms. Among them, ICP is an algorithm that does not refer to anatomical landmarks. Although scholars have verified the reliability and repeatability of the ICP algorithm when used for constructing SRPs with data from patients with normal facial symmetry, facia asymmetry data affects the algorithm's performance and makes the construction of SRPs unfeasible for patients with severe asymmetry. Scholars have since improved the global ICP algorithm by manually selecting facial regions with good symmetry for the original and mirror models; the clinical suitability of this modified ICP algorithm has improved to some extent[26, 27]. This algorithm is called the regional ICP algorithm. Although the regional ICP algorithm reduces the degree of automation by introducing human involvement, research has shown that the regional ICP algorithm is suitable for use in oral clinics. Therefore, the regional ICP algorithm, which has been screened by experts, was used as the ground truth in this study to evaluate the accuracy of our proposed algorithm.

The significant difference between the PA and ICP algorithms is that SRP extraction using the PA algorithm relies more on anatomical facial landmarks, which is consistent with clinical diagnosis and treatment. Some scholars have confirmed that the PA algorithm has a good applicability for symmetry patients, but similarity to ICP algorithm, asymmetry PA landmarks will have a Pinocchio effect on the PA algorithm[28].

One source of improvement is to filter PA landmarks. Some scholars have sorted landmarks through the recursive PA algorithm, deleting the obvious asymmetric landmarks (outliers) and using the remaining landmarks for PA operation to avoid the interference of asymmetric landmarks[29]. However, for patients with complex facial deformities (in which most of the landmark symmetries are not ideal), this algorithm may eliminate too many landmarks and tend to be locally over-optimised.

Our study proposes another way to improve the standard PA algorithm, which is to add a weighted system. We hypothesised that by analysing the distance between the corresponding original and mirror landmarks after the initial alignment, the degree of symmetry of the landmarks could be evaluated quantitatively and used as landmark weight factors to construct an SRP with personalised feature weight assignments. The WPA algorithm developed in this study did not have a reduced degree of automation caused by human intervention and could therefore simulate the expression of the reference value weight of anatomical landmarks assigned according to clinical experience. Our study showed that this was advantageous with regard to SRP construction, and our results indicated that the WPA algorithm was suitable for patients with complex mandibular deviation. However, the WPA algorithm tested in this study had some limitations.

First, the quantitative indicator of asymmetry of the landmarks (the reciprocal of the distance between paired landmarks) was indirectly obtained; to set the key parameters for the landmark weight factors, the

global ICP algorithm was used to initialise the registration of the original and mirror models. A potential way to address this limitation is to use an intelligent landmark weighting strategy based on direct morphological feature analysis, artificial intelligence, and deep learning technology, which can further improve the accuracy and rationality of landmark weight distribution and lead to better SRP constructions that simulate expert clinical diagnosis.

Second, only cases of mandibular deviation between 5 mm and 23 mm were quantitatively analysed in this study, and sample cases need to be further expanded to analyse the statistical and measurement suitability of our method for different types and degrees of facial deformities in order to provide guidance for clinical application. Therefore, testing our method on samples representing a wider range of facial deformities is a necessary area of further research.

5. Conclusions

The WPA SRP was more closely aligned than the standard PA SRP with the ground truth plane in terms of angle error, FAI error, and global and regional position error, indicating that our novel method of assigning weights to facial landmarks was an accurate way to construct an SRP for patients with facial asymmetry. We also established the position error as an effective SRP analysis tool for facial asymmetry data. Our proposed method and findings may be used to inform stomatological clinical practices for mandibular deviation diagnosis and treatment. In addition, the new method is not restricted to three-dimensional facial data, it can also be applied to skeletal models in the follow-up study, which provides a new solution for dental clinic.

Abbreviations

SRP: Symmetry Reference Plane; FAI: Facial Asymmetry Index; WPA: Weighted Procrustes Analysis; PA: Procrustes Analysis; ICP: iterative closest point; 3D: Three dimensional

Declarations

Ethics approval and consent to participate

This study was approved by the Biomedical Ethics Committee of Peking University School and Hospital of Stomatology (No: PKUSSIRB-20163113). We declare that written informed consent was obtained from all participants included in the study.

Consent for publication

Written informed consent to publish individual person’s images were obtained.

Availability of data and materials

The datasets used and analyzed during the current study are available from the corresponding author on reasonable request.

Competing interests

The authors declare that they have no competing interests.

Funding

We wish to thank the National Natural Science Foundation of China (81870815) for purchasing experimental equipment of Face Scan 3D sensor system. Key R&D Program of Ningxia Hui Autonomous Region of China (2018BEG02012) and Open Subject Foundation of Peking University Hospital of Stomatology (2019kaifangfu). The funds were used for collection, analysis, interpretation of data and manuscript editing.

Acknowledgements

The authors would like to thank the oral and maxillofacial surgery department, orthodontics department, and prosthodontics department of the Peking University School and Hospital of Stomatology for collecting clinical patients.

Authors' information

[1]Center of Digital Dentistry, Peking University School and Hospital of Stomatology, No.22 Zhongguancun Avenue South, Haidian District, Beijing 100081, China.[2]National Engineering Laboratory for Digital and material technology of stomatology, No.22 Zhongguancun Avenue South, Haidian District, Beijing 100081, China.[3]NHC Key Laboratory of Digital technology of stomatology, No.22 Zhongguancun Avenue South, Haidian District, Beijing 100081, China. [4]Beijing Key Laboratory of Digital Stomatology, No.22 Zhongguancun Avenue South, Haidian District, Beijing 100081, China.[5]National Clinical Research Center for Oral Diseases, No.22 Zhongguancun Avenue South, Haidian District, Beijing 100081, China.[6]School of Software Engineering, Beijing University of Posts and Telecommunications, No.10 Xitucheng Road, Haidian District, Beijing, 100876, China.[7]Key Laboratory of Trustworthy Distributed Computing and Service, Ministry of Education, Beijing University of Posts and Telecommunications, No.10 Xitucheng Road, Haidian District, Beijing, 100876, China.

Authors' contributions

YZhu performed data collection, statistical analysis and interpretation of results, drafted and revised the final manuscript. SZheng, GYang and XFu participated in study design and provided algorithm programming support. YZhao and YWang made substantial contributions to the conception and design

of this study, and made a critical revision of the manuscript. All authors have reviewed and agreed to the submission of the final manuscript.

References

1. Fang JJ, Tu YH, Wong TY, Liu JK, Zhang YX, Leong IF, Chen KC. Evaluation of mandibular contour in patients with significant facial asymmetry. Int J Oral Maxillofac Surg. 2016;45(7):922–31.
2. Hsu SS, Gateno J, Bell RB, Hirsch DL, Markiewicz MR, Teichgraeber JF, Zhou X, Xia JJ. Accuracy of a computer-aided surgical simulation protocol for orthognathic surgery: a prospective multicenter study. Journal of oral maxillofacial surgery: official journal of the American Association of Oral Maxillofacial Surgeons. 2013;71(1):128–42.
3. Hwang HS, Hwang CH, Lee KH, Kang BC. Maxillofacial 3-dimensional image analysis for the diagnosis of facial asymmetry. American Journal of Orthodontics Dentofacial Orthopedics. 2006;130(6):779–85.
4. Berssenbruegge P, Lingemann-Koch M, Abeler A, Runte C, Jung S, Kleinheinz J, Denz C, Dirksen D. Measuring facial symmetry: a perception-based approach using 3D shape and color. Biomedizinische Technik Biomedical Engineering. 2015;60(1):39–47.
5. Philipp MM, Angelika SE, Ute B, Jutta H, Janka K. Three-dimensional perception of facial asymmetry. Eur J Orthod. 2011;33(6):647–53.
6. Verhoeven T, Xi T, Schreurs R, Bergé S, Maal T. Quantification of facial asymmetry: A comparative study of landmark-based and surface-based registrations. Journal of Cranio Maxillofacial Surgery. 2016;44(9):1131–6.
7. Honrado CP, Larrabee WF. Update in three-dimensional imaging in facial plastic surgery. Curr Opin Otolaryngol Head Neck Surg. 2004;12(4):327–31.
8. Masoud MI, Neetu B, Jose CC, Amornrut M, Veerasathpurush A, Arshan H, Hawkins HC, Erik OC. 3D dentofacial photogrammetry reference values: a novel approach to orthodontic diagnosis. Eur J Orthod. 2016;39(2):215–25.
9. Liu XJ, Li QG, Tian KY, Wang XX, Zhang Y, Li ZL. Establishment and accuracy examination of gyroscope for recording and transferring natural head position. Beijing da xue xue bao Yi xue ban = Journal of Peking University Health sciences. 2014;46(1):86–9.
10. Djordjevic J, Toma AM, Zhurov AI, Richmond S. Three-dimensional quantification of facial symmetry in adolescents using laser surface scanning. Eur J Orthod. 2014;36(2):125–32.
11. Huang CS, Liu XQ, Chen YR. Facial asymmetry index in normal young adults. Orthodontics Craniofacial Research. 2013;16(2):97–104.
12. Hyeon-Shik H, Yuan D, Kweon-Heui J, Gi-Soo U, Jin-Hyoung C, Sook-Ja Y. Three-dimensional soft tissue analysis for the evaluation of facial asymmetry in normal occlusion individuals. Korean Journal of Orthodontics. 2012;42(2):56–63.

13. Al-Anezi T, Khambay B, Peng MJ, O'Leary E, Ju X, Ayoub A. A new method for automatic tracking of facial landmarks in 3D motion captured images (4D). International Journal of Oral Maxillofacial Surgery. 2013;42(1):9–18.
14. Codari M, Pucciarelli V, Stangoni F, Zago M, Sforza C. Facial thirds – based evaluation of facial asymmetry using stereophotogrammetric devices: Application to facial palsy subjects. Journal of Cranio Maxillofacial Surgery. 2016;45(1):76.
15. Xiaojing L, Qianqian L, Xiaoxia W, Ying H, Zheng X, Zili L. Automatic constructed MSP of 3D skull based on original-mirror alignment. Chinese Journal of Orthodontics. 2014;21(3):148–50.
16. Du S, Xu Y, Wan T, Hu H, Zhang X. Robust iterative closest point algorithm based on global reference point for rotation invariant registration. Plos One. 2017;12(11):e0188039.
17. Damstra J, Fourie Z, Wit MD, Ren Y. A three-dimensional comparison of a morphometric and conventional cephalometric midsagittal planes for craniofacial asymmetry. Clin Oral Invest. 2011;16(1):285–94.
18. Besl P, McKay N. Method for registration of 3-D shapes. IEEE Transactions on Pattern Analysis Machine Intelligence. 1992;14:239–56.
19. Walters M, Claes P, Kakulas E, Clement JG. Robust and regional 3D facial asymmetry assessment in hemimandibular hyperplasia and hemimandibular elongation anomalies. International Journal of Oral Maxillofacial Surgery. 2013;42(1):36–42.
20. Xiong YX, Yang HF, Zhao YJ, Wang Y. Comparison of two kinds of methods evaluating the degree of facial asymmetry by three-dimensional data. Beijing da xue xue bao Yi xue ban = Journal of Peking University Health sciences. 2015;47(2):340–3.
21. Xiong Y, Zhao Y, Yang H, Sun Y, Wang Y. Comparison Between Interactive Closest Point and Procrustes Analysis for Determining the Median Sagittal Plane of Three-Dimensional Facial Data. Journal of Craniofacial Surgery. 2016;27(2):441–4.
22. Severt TR, Proffit WR. The prevalence of facial asymmetry in the dentofacial deformities population at the University of North Carolina. The International journal of adult orthodontics orthognathic surgery. 1997;12(3):171–6.
23. Wu J, Heike C, Birgfeld C, Evans K, Maga M, Morrison C, Saltzman B, Shapiro L, Tse R. Measuring Symmetry in Children With Unrepaired Cleft Lip: Defining a Standard for the Three-Dimensional Mid-facial Reference Plane. Cleft Palate Craniofac J. 2016;53:695–704.
24. Wu J, Tse R, Shapiro LG: Learning to Rank the Severity of Unrepaired Cleft Lip Nasal Deformity on 3D Mesh Data. Proceedings of the IAPR International Conference on Pattern Recognition International Conference on Pattern Recognition 2014, 2014:460–464.
25. Tan W, Kang Y, Dong Z, Chen C, Yin X, Su Y, Zhang Y, Zhang L, Xu L. An Approach to Extraction Midsagittal Plane of Skull From Brain CT Images for Oral and Maxillofacial Surgery. IEEE Access. 2019;7:203–17.
26. Benz M, Laboureux X, Maier T, Nkenke E, Seeger S, Neukam FW, Häusler G: The Symmetry of Faces. In: *Vision, Modeling, & Visualization Conference: 2002*; 2002.

27. Verhoeven TJ, Nolte JW, Maal TJJ, Berge SJ, Becking AG. Unilateral Condylar Hyperplasia: A 3-Dimensional Quantification of Asymmetry. Plos One 2013, 8(3).
28. Zelditch ML, Swiderski DL, Sheets DH, Fink WL. Geometric Morphometrics of Biologists: A Primer. New York: Elsevier Academic Press; 2004.
29. Gateno J, Jajoo A, Nicol M, Xia JJ. The primal sagittal plane of the head: a new concept. International Journal of Oral Maxillofacial Surgery. 2015;45:399–405.

Table

Due to technical limitations, Table 1 is provided in the Supplementary Files section.

Figures

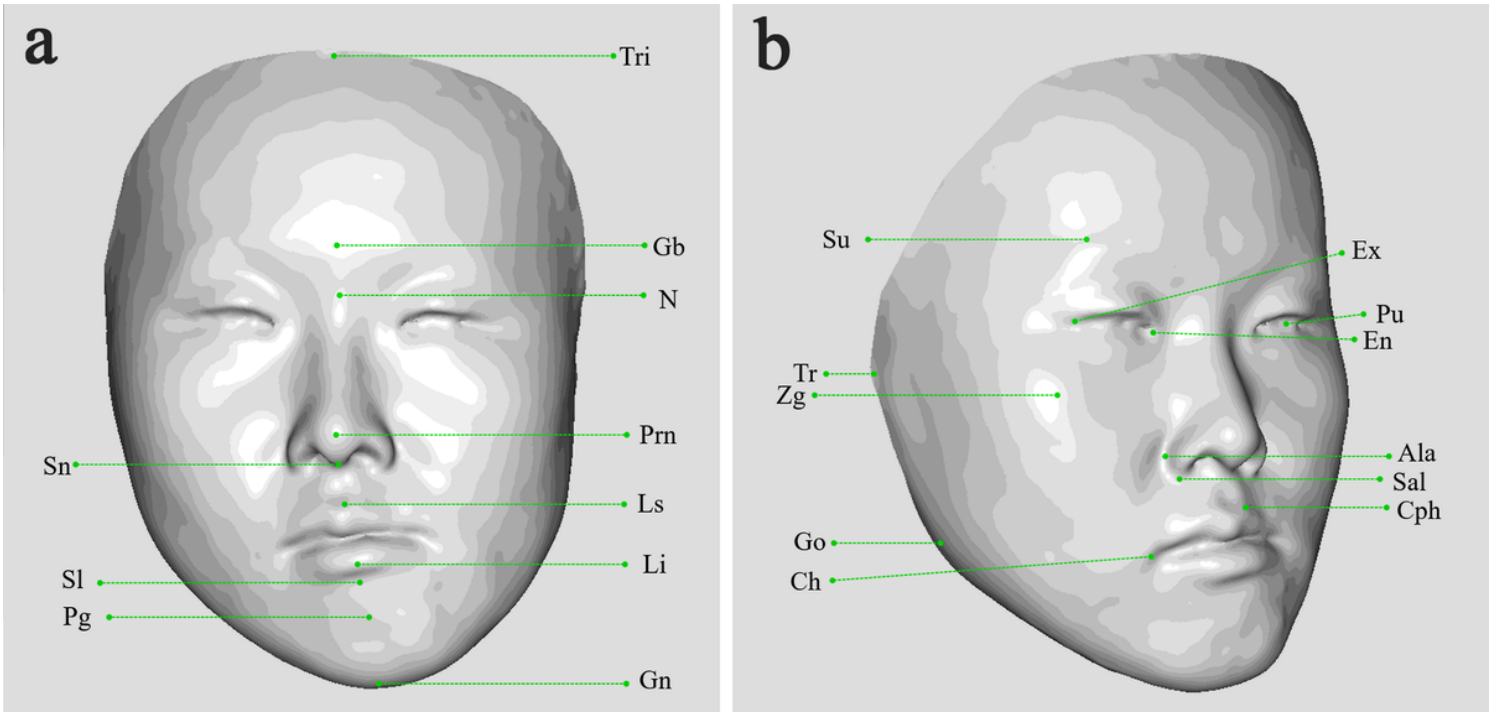

Figure 1

The 32 anatomic landmarks that are used in this study.(Upper facial third: trichion, glabella, superciliary ridge; Middle facial third: nasion, pronasale, subnasale, endocanthion, exocanthion, pupil, alare, subalare, zygion, tragion; Lower facial third : labiale superius, labiale inferius, sublabiale, pogonion, gnathion, cheilion, gonion, crista philtre).

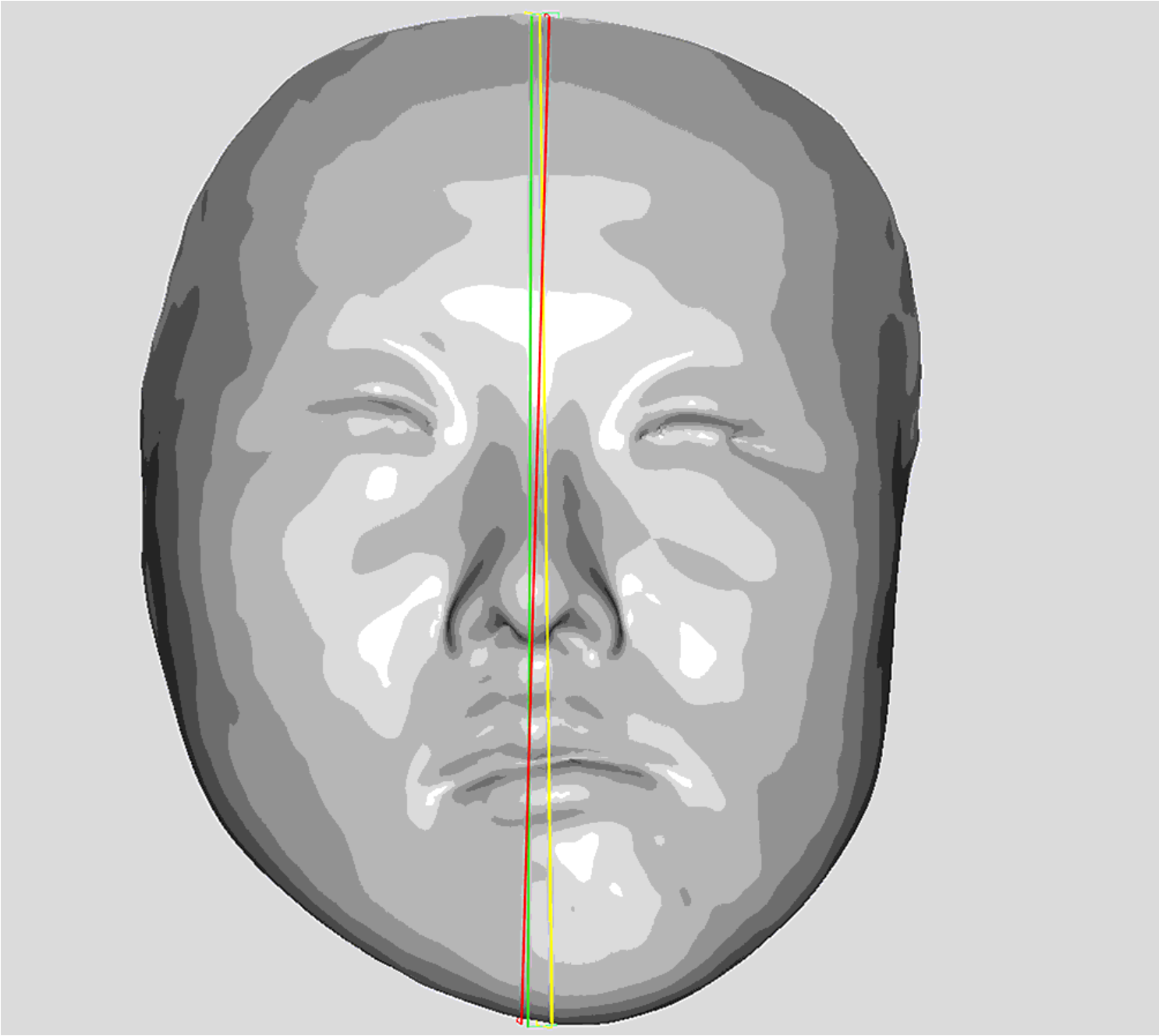

Figure 2

Abstracting the SRP based on WPA algorithm, PA algorithm and professional algorithm for one case.

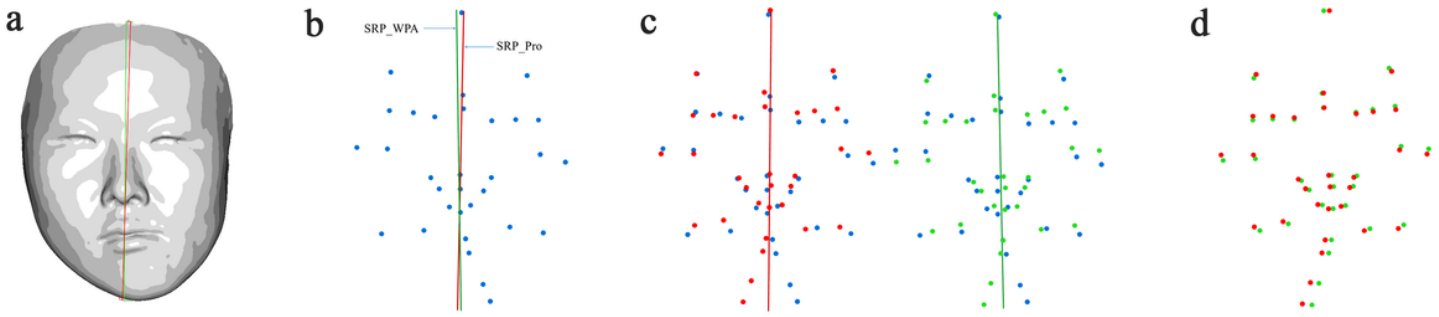

Figure 3

Position error of the mirrored landmarks. A, SRPs on original three-dimensional face, red colour plane signifies professional plane (SRP_Pro) and green colour represents WPA algorithm plane (SRP_WPA). B, Blue landmarks signify original landmarks. C, Professional mirror landmarks in red and WPA mirror landmarks in green, which were obtained from mirror original landmarks using SRP_Pro and SRP_WPA. D, Global position error was defined as the average distance of the 32 pairs of professional and WPA mirrored landmarks.

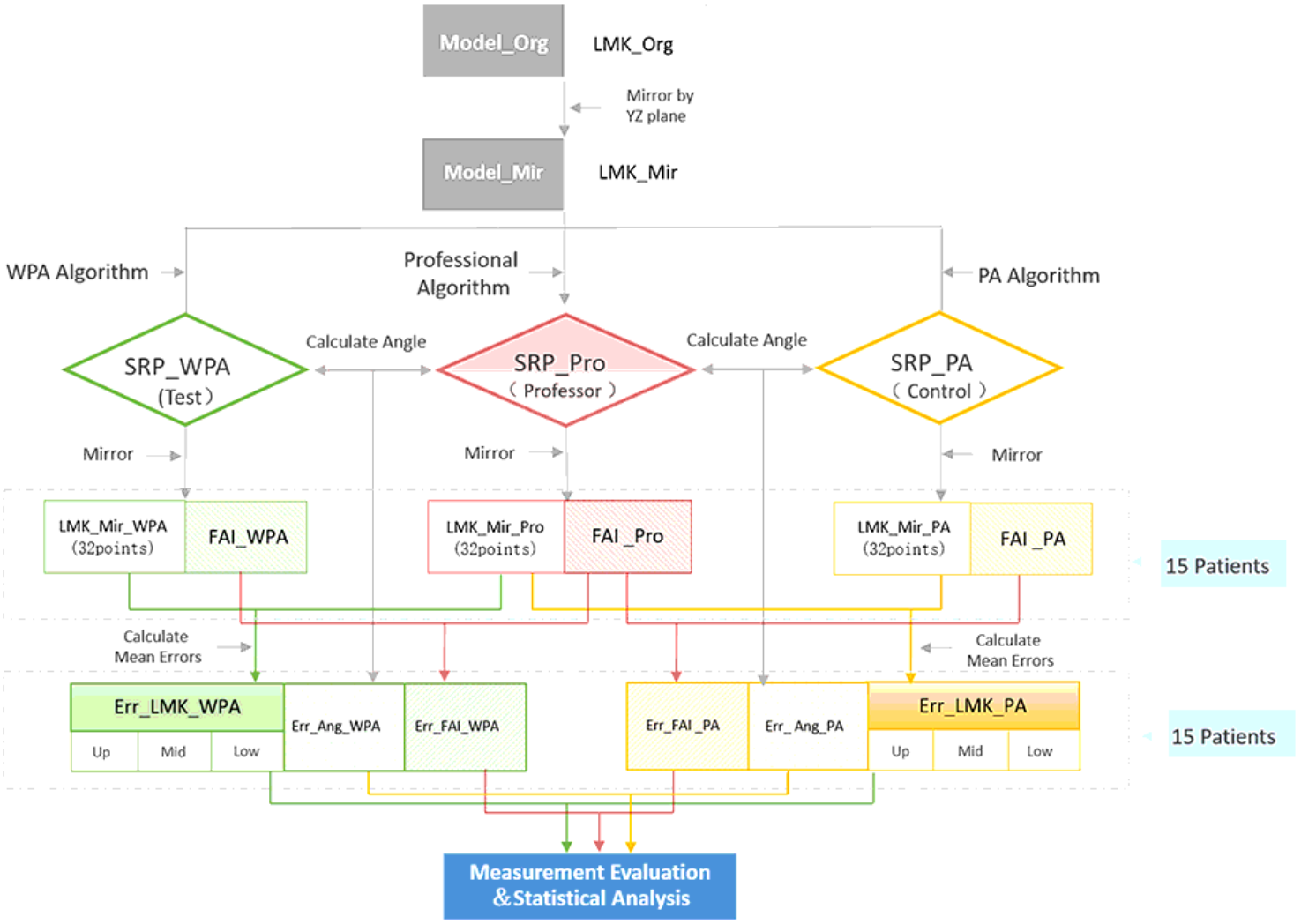

Figure 4

Workflow of the experimental procedures and evaluation methods. In the figure, WPA represents Weighted Procrustes analysis algorithm, PA represents Procrustes analysis algorithm. SRP_WPA、SRP_PA and SRP_Pro are symmetry reference planes constructed by WPA group, PA group and professional group respectively, LMK_Mir_WPA, LMK_Mir_PA and LMK_Mir_Pro are mirror landmarks constructed by WPA algorithm, PA algorithm and professional algorithm symmetry reference plane. FAI_WPA , FAI_PA and FAI_Pro are the facial asymmetry index(FAI) calculated by the SRP defined by WPA algorithm, PA algorithm and professional algorithm, Err_LMK_WPA and Err_LMK_PA are the global landmarks position errors of WPA and PA algorithms, under which Up, Mid and Low represent the position errors of different

third parts. Err_Ang_WPA and Err_Ang_PA are the angle errors of WPA algorithm and PA algorithm. Err_FAI_WPA and Err_FAI_PA are facial asymmetry index (FAI) errors of WPA algorithm and PA algorithm.

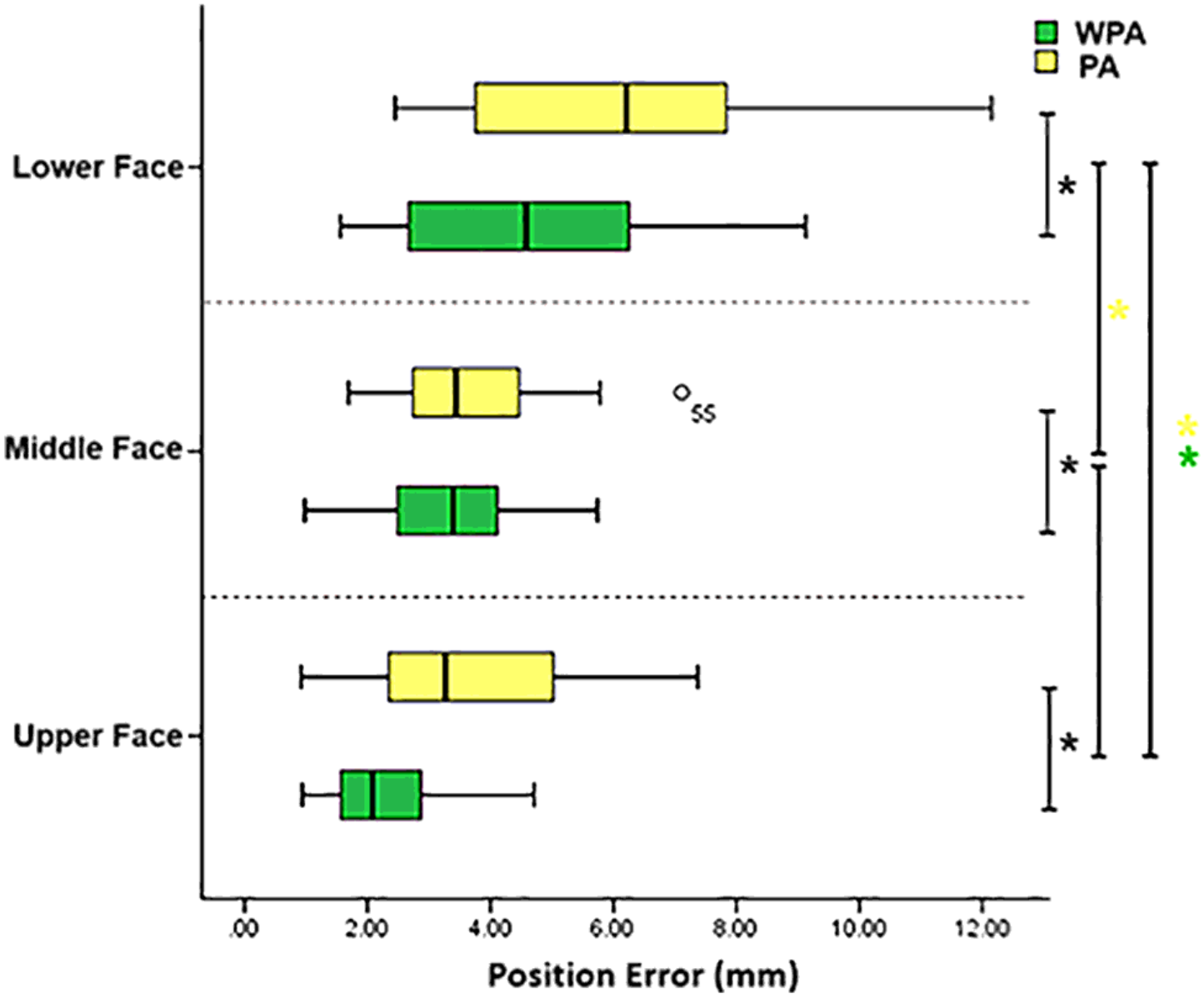

Figure 5

Boxplot of position error for upper face, middle face, lower face group. The black asterisks signify P < 0.05 between WPA algorithm and PA algorithm group. The yellow and green asterisks indicate statistical significance for position error of different regional groups using a one-way ANOVA followed by Tukey's multiple comparison test where P < 0.05, the circles within the boxplot represent outliers.

Supplementary Files

This is a list of supplementary files associated with this preprint. Click to download.

- Table.docx